Research Article

INFLUENCE OF SHOCK ABSORBER INSTALLATION ANGLE TO AUTOMOTIVE VEHICLE RESPONSE

N. Panananda[*]
S. Daowiangkan
N. Intaphrom
W. Kantapam

Department of Mechanical Engineering, Faculty of Engineering, Rajamangala University of Technology Lanna, 128 Huay-Kaew Road, Muang, Chiang-Mai, 50300, Thailand

ABSTRACT:
The installation angle of shock absorber is found theoretically to affect the damping force. In this paper, the influence of installation angle was studied numerically and experimentally. Three installation angles of 0, 45 and 90 degrees with respect to the direction of motion were considered. The base excited single degree of freedom was set up for experimental study. A single cycle sine squared base excitation was implemented to simulate the road hump. The results show that the installation angle of 0 degrees is capable to stop sprung mass vibration in the shortest time compared to other installation angles. In contrast, the installation angle of 90 degrees results in the greater mass oscillation amplitude which degrades handling quality. The installation angle of shock absorber is found to influence directly the vibration characteristic of the vehicle. The shock absorber installation angle is then another aspect for the suspension design consideration.

Keywords: *Shock absorber; Handling; Ride-comfort; Installation angle.*

1. INTRODUCTION

Automotive vehicle suspension system is required to have the characteristic corresponding to purpose of use. The passenger cars require the suspension system to be softer for the ride-comfort quality. The ride comfort quality refers to the capability of the suspension system to reduce force transferring from the wheels to passengers. So that, the passengers do not experience the discomfort resulting from the road. In contrast, the suspension system for the sport cars should be stiffer for handling quality. Handling quality refers to the capability of the vehicle to be controlled or manoeuvred. By this means, the oscillation of the vehicle and the suspension movement should be limited. Such the suspension setup can cause the passengers to experience discomfort from transferring forces the wheels. These are the trade-off between the ride-comfort and handling qualities. By improving the suspension to be more comfortable, it reduces the vehicle handling quality and vice versa.

The ride-comfort and handling qualities for the passive suspension system may not meet compromise. It depends on the purpose of the vehicle. Fig. 1 shows the recommended values of damping ratio of the shock absorber [1]. It is seen that the damping ratio for the ride-comfort quality can be around 0.2 whereas that for handling quality should be higher as 0.8. The greater number of damping ratio refers to the greater damping force being produced by the shock absorber for small relative velocity across the shock absorber. The lower damping ratio shock absorber allows greater movement of the suspension or lower damping force for the same level of relative velocity.

---

* Corresponding author: N. Panananda
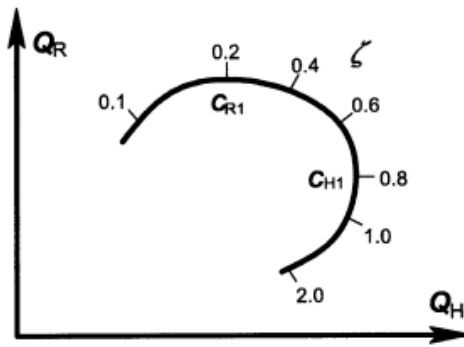E-mail address: nuttarut@rmutl.ac.th

Fig. 1. The ride-handling loop for the automotive vehicle [1].

The damping force characteristic of the automotive shock absorber, in general, does not possess a single value of damping ratio. It is usually designed to have different forces between the extension and compression strokes. Surace et al. tested the automotive vehicle shock absorber and found the characteristic as shown in Fig. 2 (a) [2], for example. The damping ratio for the compression stroke is usually less than that for the extension stroke. This is to reduce the harshness when the vehicle is passing the road bump, the shock absorber should not produce any damping force during the compression stroke. Thus damping ratio for this direction must be kept lower. This is to allow the unsprung mass, the mass underneath the suspension, to move almost freely. Thus there is low level of force transferring via shock absorber to the mass over the suspension system or the sprung mass. However, in the opposite direction, the shock absorber should produce more damping force in the extension stroke to prevent the vehicle from oscillating.
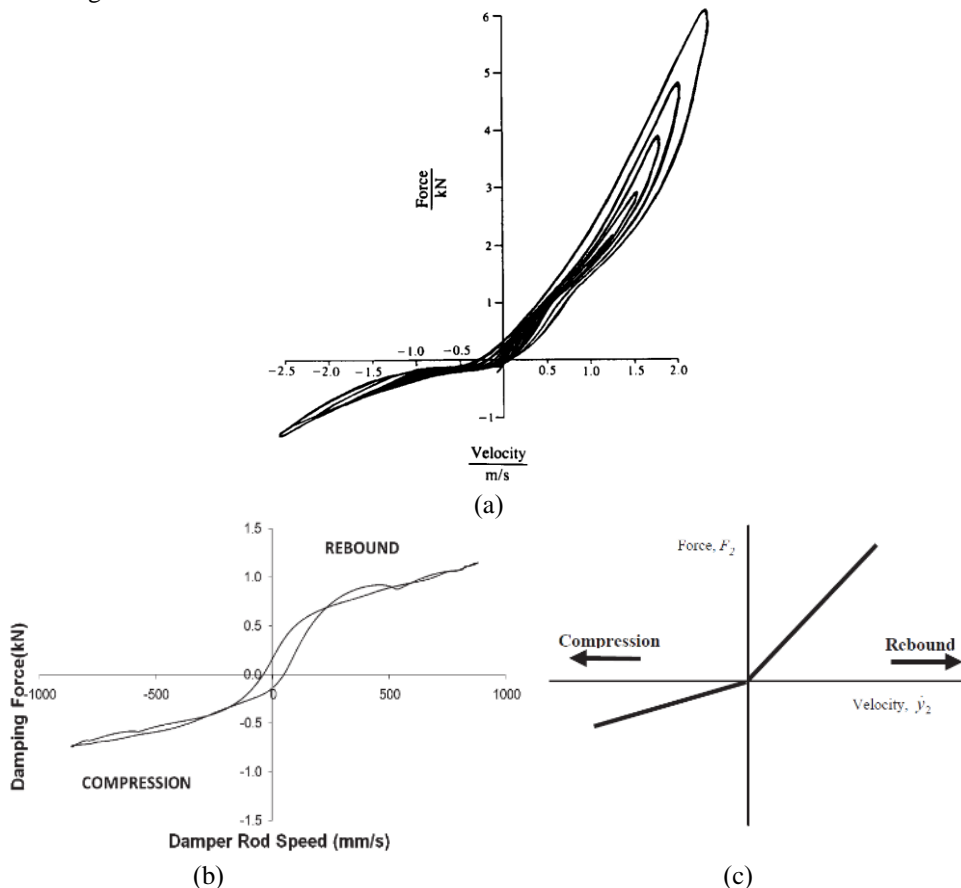

Fig. 2. Asymmetric damping force characteristic obtained by
(a) Surace et al. [2], (b) Calvo et al. [3] and (c) Rajalingham et al. [4].

Additionally, J.A.Calvo et.al. [3] experimented the vehicle shock absorber to find the damping force characteristic. The force characteristic was found in form of the piecewise linear with hysteresis loop as shown in Fig. 2 (b). The hysteresis loop was described as the effect of friction. Duym et al. [5] mentioned that the hysteretic effects is commonly known to happen at the beginning of either compression or extension stroke. The study in asymmetrical damping force characteristic has been published in similar fashion, for example, Cafferty and Tomlinson [6], Rao et.al. [7] or Worden et.al. [8]. Among these publications, found that it is suitable to represent the damping force characteristic using only the piecewise linear damping force characteristic without the hysteresis loop as applied in [4] and shown in Fig. 2 (c). Such the damping force characteristic is also assumed in this paper. Waters et.al. [9] also found that the value of damping ratios for the compression and extension strokes directly affect the response of the sprung mass. The maximum acceleration for the sprung mass was found to be reduced by reducing the damping force in the compression stroke.

Practically, the damping ratio of shock absorber can be altered by adjusting the piston valves inside the shock absorber. It is obvious that adjusting the valves results in the damping force characteristic. Since it limits the flow rate of fluid inside the shock absorber. However, in this paper, the characteristic of the shock absorber is kept unchanged. The damping force characteristic of the system in this paper is modified by the installation geometry. The damping force characteristic is commonly known to be a function of velocity across the damper. By adjusting the installation geometry, the damping force becomes the function of velocity and the displacement. Bin Tang and M.J.Brennan [10, 11] had studied and compared the force transmissibility of two systems as shown in Fig. 3. The damper was considered to be installed by 0 degree or in the direction of motion and 90 degree or perpendicular to the motion of the sprung mass. They found that the installation angle affects the vibration behaviour of the system. The perpendicular installed damper was found to reduce the vibration response at the frequencies higher than the natural frequency.

It is interesting for the effects of the damper installation geometry on the vehicle suspension system. In this paper, the vehicle suspension system is represented by a base excited vibration isolation model. The models are as shown in Fig. 4.
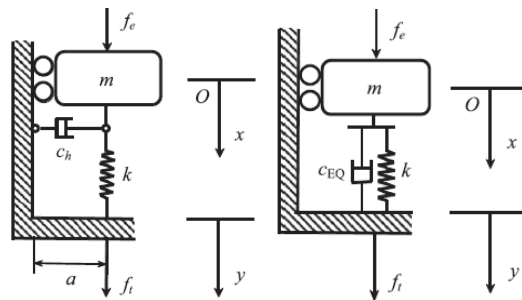

Fig. 3. The force excited vibration isolation having the damper
in different installation angles [10, 11].

2. INSTALLATION ANGLE CONFIGURATIONS

The single degree of freedom base excited vibration systems as shown in Fig. 4 are considered in this study. The installation angles are considered with the respect to the direction of motion which is the vertical direction. Equations of motion for each models can be extracted from the installation geometry by means of damping force as the free body diagrams shown in Fig. 4. The damping force function for each damping installation angle is described in the following subsections.

2.1 Vertical shock absorber

In Fig. 4 (a), the shock absorber is considered to be working in the direction of motion. For either stroke of the shock absorber, the damping force is commonly known to be a function of relative velocity across the damper, y', and is as shown in Eq. (1).

$$F_{dy} = -c_a y' \tag{1}$$

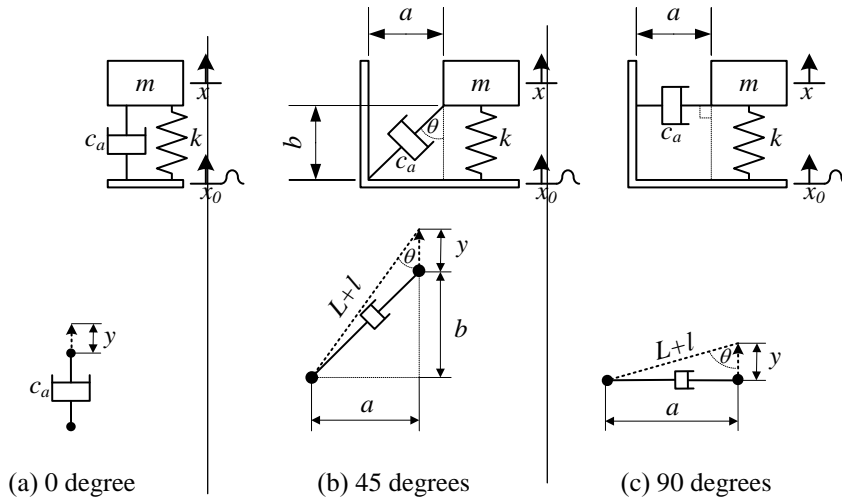where c_a is the damping coefficient of the shock absorber.

Fig. 4. Geometrical consideration for the damping force
in different installation angles.

2.2 Inclined shock absorber

The installation angle shown in Fig. 4 (b) is said to have an inclined shock absorber. The damping force can be also extracted from the free-body diagram shown in Fig. 4 (b). The free-body diagram in Fig. 4 (b) shows that the shock absorber is installed at θ degrees with respect to the direction of motion.

The free length of shock absorber is L. y represents the upward direction of the sprung mass relatively to the base excitation. The length of shock absorber becomes $L+l$. The relative velocity across the shock absorber can be then defined by taking derivative of $L+l$ and becomes l'. The damping force in the direction of motion is equal to

$$F_{dy} = F_d \cos\theta \tag{2}$$

where F_d is the damping force across the shock absorber and is defined by $F_d = -c_a l'$. By extracting the force from the free-body diagram, the damping force across the shock absorber can be given as

$$F_d = -c_a \frac{(b+y)\,y'}{\sqrt{a^2 + (b+y)^2}} \tag{3}$$

where a and b are installation geometry as shown in Fig. 4 (b). The dimension of a and b can be considered as the ratio of installation geometry. For the case that $a = 0$, it is the same as that for vertical shock absorber. So that, for the damping force in the direction of motion can be described by

$$F_{dy} = -c_a \frac{(b+y)^2}{a^2 + (b+y)^2}\,y' \tag{4}$$

Eq. (4) is seen to be function of relative velocity and relative displacement across the shock absorber. In addition, parameters a and b play the important role. By having $a \to 0$, Eq. (4) becomes function of relative velocity as that in Eq. (1). When $b \to 0$, the shock absorber is considered to be installed horizontally to the direction of motion.
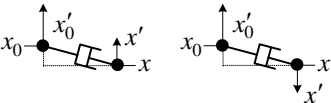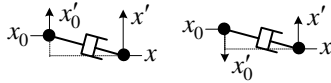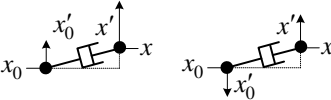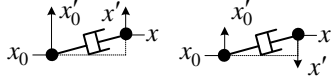
2.3 Horizontal shock absorber

The shock absorber in horizontal installation angle is as shown in Fig. 4 (c). The damping force in the direction of motion, F_{dy}, can be described by extracting the free-body diagram shown in Fig. 4 (c) and can be described as

$$F_{dy} = -c_a \frac{y^2}{a^2 + y^2} y' \tag{5}$$

It is seen in Eq. (5) that there is no parameter b for the horizontal installed shock absorber. The damping force depends only on the length of the shock absorber. The longer shock absorber can result in the lower level of damping force. Moreover, the damping force is seen to be a function of relative velocity and relative displacement similar to the inclined configuration shock absorber.

Additionally, the damping force for the horizontal installation angle is different from the previous two installation angles regarding the piecewise damping force characteristic. The shock absorber installed in vertical or inclined geometry is in the extension stroke whenever the system mass is moving greater than the base. As a result, the greater level of damping force is produced for such the movement.

Table 1: Damping force produced for the horizontal damping configuration

Extension (Higher damping force)	Compression (Lower damping force)
$x_0 \geq x$ and $x_0' \geq x'$	$x_0 \geq x$ and $x_0' \leq x'$
$x_0 \leq x$ and $x_0' \leq x'$	$x_0 < x$ and $x_0' > x'$

This is in contrast to the shock absorber installed horizontally. The damping force is produced in the total different ways from the other two configurations. For the horizontal installation angle, the production of the damping force can be described as listed in Table 1. The shock absorber will be in the extension direction for two conditions. It will be in extension stroke when either the displacement and the velocity of base excitation, x_0 and x_0', are greater than those of the mass or the displacement and the velocity of base excitation are lower than those of the mass, x and x'.

The shock absorber is producing the damping force in compression direction for either of the following cases, excitation base is in greater displacement but lower velocity than those of the mass or excitation base is in lower displacement but greater velocity than those of the mass. This can be described graphically as shown in Table 1.

3. MATHEMATICAL MODELS AND NUMERICAL SIMULATIONS

By considering the damping force configurations in previous section, the mass normalised equation of motion can be given as shown in Eqs. (6) to (8) for the installation angle of 0 degree, 45 degrees and 90 degrees respectively.

$$y'' + 2\omega_n \left(\zeta_s + \zeta_a \right) y' + \omega_n^2 y = -x_0'' \tag{6}$$

$$y'' + 2\omega_n \left(\zeta_s + \zeta_a \frac{(b+y)^2}{a^2 + (b+y)^2} \right) y' + \omega_n^2 y = -x_0'' \tag{7}$$

$$y'' + 2\omega_n \left(\zeta_s + \zeta_a \frac{y^2}{a^2 + y^2} \right) y' + \omega_n^2 y = -x_0'' \tag{8}$$

In this study, a and b were set to be equal, i.e., the installation angle of 45 degrees was performed. ζ_s is the equivalent viscous damping ratio resulting from other effects of the system. ζ_a and ω_n are the shock absorber damping ratio and system natural frequency. y, y' and y'' are displacement, velocity and acceleration of the relative motion across the damper which is determined from the relative motion, i.e., $y = x - x_0$.

The base excitation was assumed to be a sinusoidal squared road hump. The hump has the shape and dimensions as shown in Fig. 5 (a). However, the dimensions of the base excitation for this study was modified to be in accordance with the experimental study but still be in the shape of sinusoidal squared. The new dimensions are as shown in Fig. 5 (b). It was assumed to have the vehicle running over the hump within 0.3125 seconds.
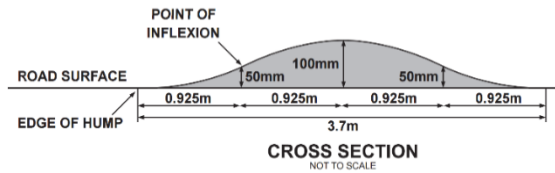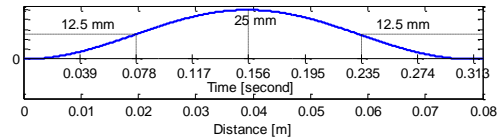
(a)   (b)

Fig. 5. (a) The sinusoidal road hump base excitation [12] and (b) The numerical base excitation.

The mathematic models shown in Eqs. (1) – (3) were solved numerically. Numerical simulation employed in this study was done using ODE4 with the fixed time step of 1 millisecond. The base input and the system mass response were applied as the acceleration. The numerical results in the form of acceleration are compared to the experimental results. The asymmetric damping force was also applied for numerical simulation. The damping ratio applied for numerical simulation were 0.8 and 0.6 for extension and compression strokes, respectively.

4. EXPERIMENTAL SETUP

The experimental study was carried out in order to validate the numerical simulation. The experimental rig was designed as a base excited single degree of freedom, as the drawing shown in Fig. 6. It consisted of a system mass, a suspension spring and two shock absorber. The base excitation was implemented using an eccentric driving mechanic. The eccentric cam was located at one end of the rig frame. The other end of the frame connected to the pivot joint. So the frame was acting as the wheel being on the road hump. The eccentric cam was designed to perform the sinusoidal squared as shown in Fig. 6.
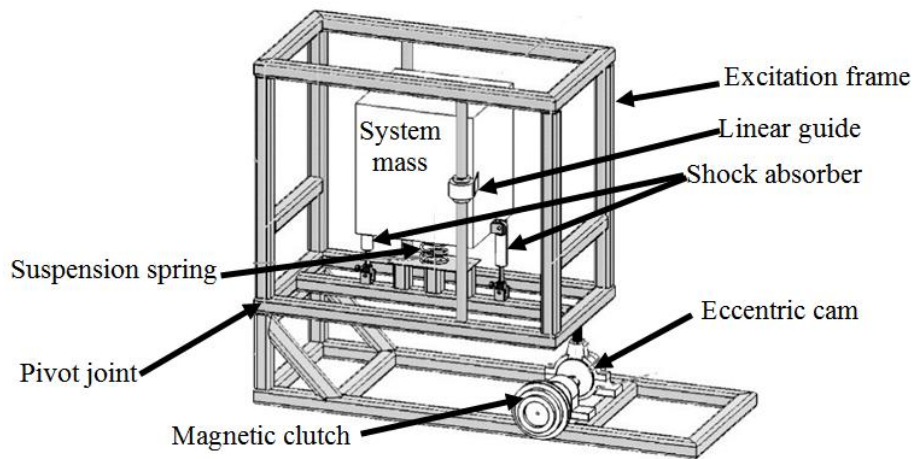
Fig. **6**. The experimental rig.

The eccentric cam was driven by an electric motor. The shaft of the electric motor connected to a magnetic clutch. The magnetic clutch was forced to operate when the motor reached the desired rotational speed of 3.2 Hz. The magnetic clutch then connected and transmitted power from the electric motor to the eccentric cam for 1 revolution. It took around 0.3125 seconds to complete a cycle. At this stage, the frame was driven as the profile shown in Fig. 7. The system mass was constrained to be moving in only the vertical direction. The mass was guided vertically using the linear bearings as shown in Fig. 6.

The shock absorber employed in this study was the adjustable mono-tube shock absorber for mountain bike as shown in Fig. 8 (a). The length of the shock absorber from end to end is 160 mm and 130 mm for fully extended and fully compressed, respectively. The maximum travelling distance of the shock absorber is around 30 mm. However, only 15 mm was considered for the experiment.
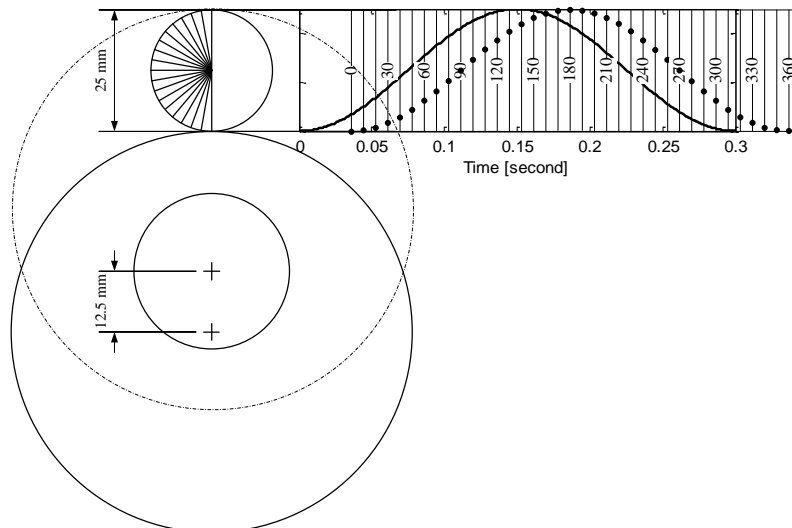

Fig. **7**. Sinusoidal squared profile for eccentric cam.

The shock absorbers were tested to obtain the damping force characteristic. The different frequencies sinusoidal excitation with constant displacement of 15 mm were applied to obtain the damping force for each frequency. The damping force characteristic are as shown in Figs. 8 (b) and (c). It appeared asymmetric with higher force for extension stroke with the damping coefficient of around 390 N-s/mm and 332 N-s/mm. The compression stroke

appeared to have the damping coefficient of around 292 N-s/mm and 242 N-s/mm. Thus the average calculated values of damping ratio, ζ_a, were about 0.2 for extension stroke and 0.15 for compression stroke.
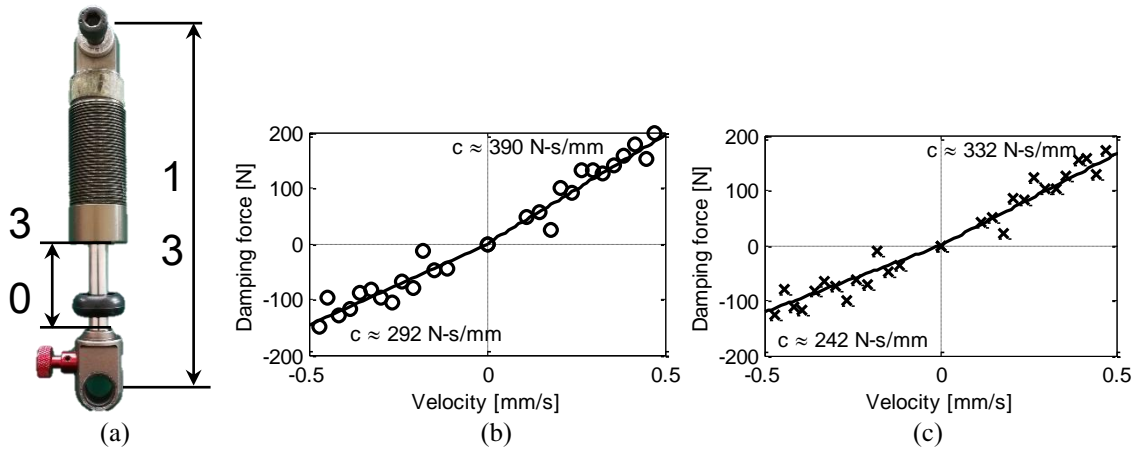

Fig. 8. (a) Shock absorber; (b) and (c) Damping force characteristic.

The system natural frequency was assumed initially to be 4 Hz or 8π radian/second. This is due to the limitation of signal acquisition equipment in acquiring the very low frequency signals. The mass of the system was set to be 40 kg. Thus calculated stiffness of the suspension spring was calculated to be 25.266 kN/m. The suspension spring with the dimension shown in Fig. 9 was designed. However, the stiffness of the actual spring was around 23.077 kN/m. As such the natural frequency of the system was around 3.8 Hz.
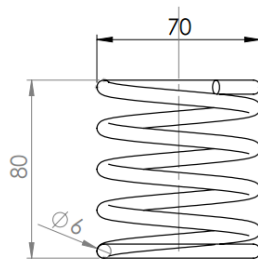

Fig. 9. Dimension of the system spring.

The shock absorber was installed in three different angles, i.e., 0, 45 and 90 degrees. The installation angles are as shown in Fig. 10. Two accelerometers were attached at the frame and the centre on top of the system mass. The accelerations for both, system mass and base excitation, were captured using the B&K accelerometers type 4519-003. The accelerometer has an ability to capture the signal in the frequency range of 1 Hz to 20 kHz, and has the mass of 1.5 grams. The accelerometers were attached at the top centre of the mass and the bottom centre of the base excitation, approximately in the same vertical alignment.
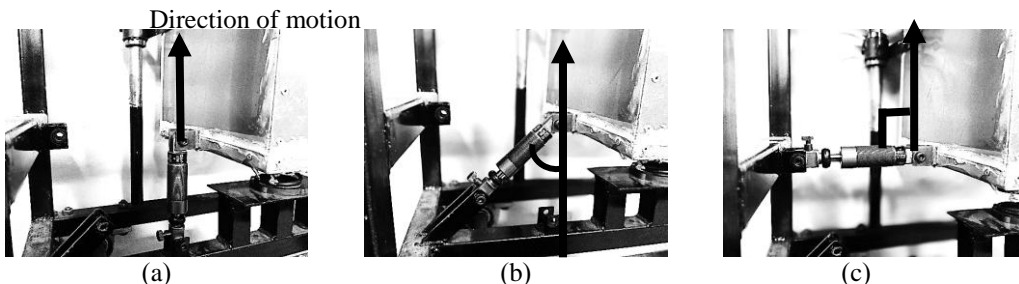

Fig. 10. Installation angles with (a) 0 degree, (b) 45 degrees and (c) 90 degrees.

5. RESULTS AND DISCUSSIONS

The numerical results and experimental results are compared as shown in Fig. 11. It also shows the comparison of the responses for different installation angles. The thin solid line represents the input acceleration which obtained from experimental data. This acceleration excitation was applied for the numerical simulation. The thick solid lines represent the experimental results whereas the dashed lines represent the numerical simulation.

Firstly, the experimental results are examined. It is seen in Fig. 11 that the installation angle of 0 degree provided the lowest acceleration peak with the shortest oscillating time. The installation angle of 45 degrees and 90 degrees respectively resulted in higher acceleration peaks and longer oscillating time. The highest accelerations for the experimental results are about 3.9 m/s^2, 5.2 m/s^2 and 8.4 m/s^2 for 0, 45 and 90 degrees installation angles respectively. It is noticed that the system mass for 90 degrees installation angle was still oscillating for around 0.6 second. It reached the equilibrium position at around 1 second as shown in the Fig.11. Whereas 0 degree and 45 degrees installation angles limit the oscillation period in less than 0.2 seconds, i.e. $0.4 - 0.6$ seconds.

Secondly, results obtained using numerical simulation are compared to the experimental results. The mathematical model shown in Eqs. (6) – (8) were employed. The results are seen to follow the experimental results appropriately with the coefficient of determination, R^2, of about 0.85, 0.86 and 0.89, respectively. The numbers of R^2 show the appropriate linear relationship between the numerical and experimental results. This can be implied that the responses of the vehicle having different installation angles for shock absorber could be interpreted using the mathematic models. The effects of installation angle could also be examined appropriately using numerical simulation.
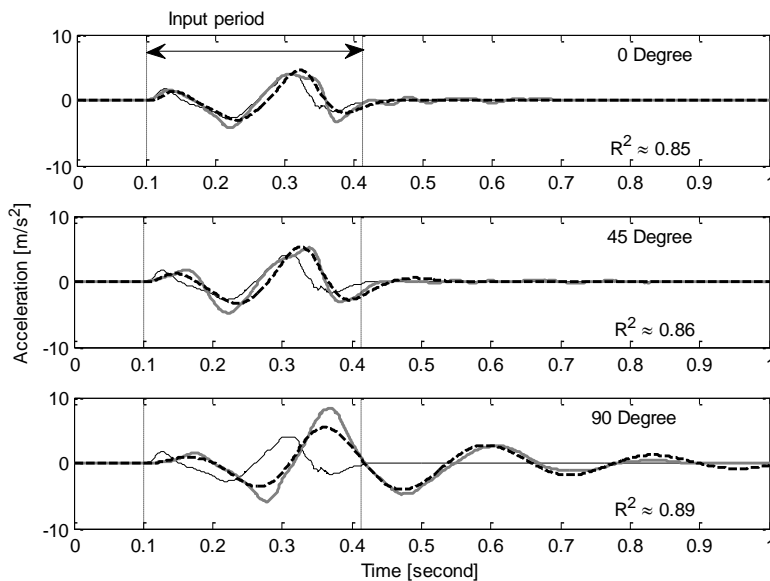

Fig. 11. Time responses in comparison between the experimental and numerical results.

The effects of installation angle are examined by means of system mass acceleration, relative velocity and damping force obtained from numerical simulation. Only the model shown in Eq. (7) was employed at this stage. The installation angle applied in numerical simulation was varied from 0 to 90 degrees with 1 degree resolution by varying the parameters a and b. Fig. 12 (a) shows comparison of the peak acceleration obtained from experiment,

represented using circle markers, and numerical simulation. It is seen that the peak acceleration is higher for the greater installation angle. The results from both, experiment and numerical simulation, are in good agreement.

The peak relative velocity shown in Fig. 12 (b) is also employed to examine the effects of installation angle. It is seen that, for both experimental and numerical results, the installation angle of 0 degree provided the lowest relative velocity. This can be the consequence result of low acceleration of the sprung mass whereas that for 90 degrees installation is the highest. However, when the damping force is considered. It is seen that the highest level of damping force can be obtained for installation angle of 0 to around 20 degrees. Whereas that for 90 degrees installation angle appears about no damping force. This can be interpreted using the installation geometry shown in Fig. 4. The installation of 0 degree obtains the damping force directly from the vertical motion. In contrast for that for 90 degrees, the damping is produced in comparatively small level. It is also seen in Eq. (5) that the greater of parameter a results in the much lower damping force.

To this point, the effects of installation angle can be concluded. For the improvement of handling quality, the shock absorber should be installed in the same direction of motion. This is to obtain the maximum level of damping force. Therefore, the sprung mass oscillation is limited. On the other hand, to avoid the force transferring to the passengers, the shock absorber should be installed horizontally to the direction of motion. By doing so, the transferring force is kept minimum but the sprung mass is oscillating the most. Thus it is dependent on the purpose of the vehicle. The designer must be careful for such consideration. Fig. 12 can be used to assist to design the shock absorber installation angle.
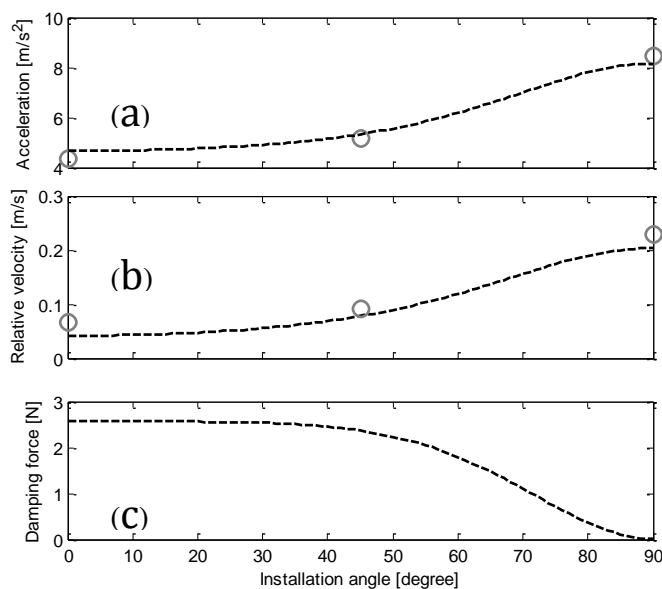

Fig. 12. Peak values for (a) acceleration (b) relative velocity and (c) damping force
○ experimental results, ------ numerical simulation.

6. CONCLUSION

This research paper reveals the effects of installation angle for the automotive vehicle shock absorber. The experimental study was implemented to obtain the response of the sprung mass. The sinusoidal shape road hump was applied to excite the system. The system was excited by a single cycle of the eccentric cam. The response of the sprung mass was captured and examined in comparison to the results obtained from numerical simulation. Three installation angles were applied consequently to the experimental study, i.e., 0, 45 and 90 degrees with respect to the

direction of motion. The results obtained from both experimental and numerical simulation are in good agreement. Then, other installation angles were applied for the numerical simulation to get the trend of responses. It is found that the installation angle of 0 degrees provides the lowest oscillation of the sprung mass but the highest damping force transfer. Thus this installation angle is better to improve the handling quality. This is in contrast to installation angle of 90 degrees for which there is almost no damping force to the sprung mass. However, it results in the maximum oscillation of the sprung mass. These results show that, apart from the shock absorber characteristic, trade-off between handling and ride quality can be improved by considering the shock absorber installation angle. However, these results just show the effects of installation angle for a single speed. It is also interesting to examine the influence of the shock absorber installation angle for the variable speeds and also the variable shape of road input.

NOMENCLATURE

a	horizontal geometrical dimension, m
b	vertical geometrical dimension, m
c_a	damping coefficient for shock absorber, N-s/m
k	suspension spring stiffness, N/m
m	system mass, kg
x , x'	absolute displacement and velocity for the system mass, m and m/s
x_0 , x_0'	absolute displacement and velocity for the base excitation, m and m/s
y , y'	relative displacement and velocity between the system mass and base excitation, m and m/s
F_d	damping force, N
F_{dy}	damping force in y direction, N
ω_n	natural frequency of the system, rad/s
ζ_s	damping ratio from other condition
ζ_a	damping ratio from shock absorber

REFERENCES

[1] Dixon, J. C. The Shock Absorber Handbook, 2nd Edition, 2007, John Wiley & Sons, England.

[2] Surace, C., Worden, K. and Tomlinson, G. R. On the non-linear characteristics of automotive shock absorbers, Proceedings of the Institution of Mechanical Engineers, Part D: Journal of Automobile Engineering, Vol. 206(1), 1992, pp. 3-16.

[3] Calvo, J. A., López-Boada, B., Román, J. L. S. and Gauchía, A. Influence of a shock absorber model on vehicle dynamic simulation, Part D: Journal of Automobile Engineering, Vol. 223(2), 2009, pp. 189-203.

[4] Rajalingham, C. and Rakheja, S. Influence of suspension damper asymmetry on vehicle vibration response to ground excitation, Journal of Sound and Vibration, Vol. 266(5), 2003, pp. 1117-1129.

[5] Duym, S., Stiens, R. and Reybrouck, K. Evaluation of shock absorber models, Vehicle System Dynamics, Vol. 27(2), 1997, pp. 109-127.

[6] Cafferty, S. and Tomlinson, G. R. Characterization of automotive dampers using higher order frequency response functions, Proceedings of the Institution of Mechanical Engineers, Part D: Journal of Automobile Engineering, Vol. 211(3), 1997, pp. 181-203.

[7] Rao, M. D., Gruenberg, S. and Torab, H. Measurement of Dynamic Properties of Automotive Shock Absorbers for NVH, In Proceedings of the 1999 Noise and Vibration Conference, SAE Technical Paper 1999-01-1840.

[8] Worden, K., Hickey, D., Haroon, M. and Adams, D. E. Nonlinear system identification of automotive dampers: A time and frequency-domain analysis, Mechanical Systems and Signal Processing, Vol. 23(1), 2009, pp. 104-126.

[9]   Waters, T. P., Hyun, Y. and Brennan, M. J. The effect of dual-rate suspension damping on vehicle response to transient road inputs, Journal of Vibration and Acoustics, Vol. 131(1), 2009, pp. 011004-011004.

[10]   Tang, B. and Brennan, M. J. A comparison of two nonlinear damping mechanisms in a vibration isolator, Journal of Sound and Vibration, Vol. 332(3), 2013, pp. 510-520.

[11]   Tang, B. and Brennan, M. J. A Comparison of the Effects of Nonlinear Damping on the Free Vibration of a Single-Degree-of-Freedom System, Journal of Vibration and Acoustics, Vol. 134(2) 2012, p. 024501.

[12]   Traffic Calming, Local Transport Note 1/07, Department for Transport, 2007, London, UK.